Neuroscience Vol. 41, No. 2/3, pp. 365–379, 1991
Printed in Great Britain

0306-4522/91 $3.00 + 0.00
Pergamon Press plc

THALAMOCORTICAL RESPONSES OF MOUSE SOMATOSENSORY (BARREL) CORTEX *IN VITRO*

A. AGMON*† and B. W. CONNORS‡§

*Department of Neurology, Stanford University School of Medicine, Stanford, CA 94305, U.S.A.
‡Section of Neurobiology, Box G, Division of Biology and Medicine, Brown University, Providence, RI 02912, U.S.A.

Abstract—We have developed a novel slice preparation of the mouse somatosensory forebrain. This preparation is unique in including both the ventrobasal nucleus of the thalamus and the sensorimotor "barrel" cortex in a 400-μm-thick slice with the functional connectivity between them preserved, and in allowing direct visualization of the various components of the barrel system in unstained living tissue. Thalamocortical connectivity was demonstrated by recording the laminar profile of cortical field potentials evoked electrically from the ventrobasal nucleus. Current-source density analysis of this profile showed that the largest and earliest sinks were coextensive with the two known sites of thalamocortical terminals, layer IV and the junction of layers V and VI. The sink in layer IV could be dissociated experimentally into a small, early sink of presynaptic origin (most probably a presynaptic spike volley in the thalamocortical terminals) and a later, larger sink generated postsynaptically. By mapping the subcortical stimulation sites that elicited a response at different layer IV recording sites we concluded that the thalamus-to-cortex projection preserves the general dorsoventral relationship of the afferents. Intracellularly recorded responses elicited by thalamic stimulation included (but were not limited to) monosynaptic excitatory and disynaptic inhibitory postsynaptic potentials. The thalamus-to-cortex connections were also mapped with the axonal fluorescent tracer dioctadecyl-tetramethylindocarbocyanine perchlorate.

The thalamocortical slice is a very suitable system for studying the physiology and pharmacology of the thalamocortical synapse and for exploring the synaptic circuitry of the somatosensory cortex.

Rodent somatosensory cortex has received increasing attention during the past two decades due to a unique property: the vibrissae representation in layer IV consists of discrete clusters of cell bodies called "barrels" that, viewed in a tangential plane, form a topological replica of the whisker pad.[55] Moreover, each barrel receives its main sensory input from its corresponding vibrissa.[48,49] This striking structure–function relationship makes the barrel cortex a particularly attractive system for studying sensory information processing in the neocortex and the synaptic circuitry underlying it. Using electron-microscopic techniques, White and coworkers have conducted detailed studies of thalamocortical and other synaptic contacts made on a variety of cell types in the barrel cortex.[50] Other workers have investigated topographical organization and receptive field properties in the barrel cortex.[6,9,10,21,41–43]

The rodent somatosensory cortex has also been studied *in vitro*.[12] The slice preparation allows visually guided access to the tissue for recording, stimulation and drug application, control over the ionic composition of the extracellular space, and enhanced mechanical stability during intracellular recordings and dye fillings. Application of these methods to the rodent neocortex has uncovered a previously unrecognized diversity of electrophysiological cell types within it.[4,11,31] However, the slicing methods used so far have resulted in truncation of all afferent and efferent connections with subcortical structures, a major limitation when studying neuronal circuitry. The results have previously been reported in abstract form[2,3] and in a dissertation.[1]

EXPERIMENTAL PROCEDURES

Preparation and maintenance of thalamocortical slices

The animals used were two- to five-week-old black mice (C57 BL/6, either sex, Simonsen), except for the dioctadecyl-tetramethylindocarbocyanine perchlorate (Di-I) experiment, which used an 11-day-old animal. To prepare slices, an animal was anesthetized with halothane, decapitated, and the bones and dura mater covering the cortical surface were carefully peeled away. The brain anterior to the tectum was removed and placed on a 10° ramp made from a glass slide glued to two plexiglass triangles. The tissue was placed with the ventral face toward the glass slide and the anterior end downhill (Fig. 1A). Throughout this and the following procedures the exposed brain surface was frequently irrigated with ice-cold artificial cerebrospinal fluid (ACSF; see below for composition) saturated with a 95:5 O_2–CO_2

†Present address: Department of Anatomy and Neurobiology, California College of Medicine, Irvine, CA 92717, U.S.A.
§To whom correspondence should be addressed.

Abbreviations: ACSF, artificial cerebrospinal fluid; CSD, current-source density; Di-I, dioctadecyl-tetramethylindocarbocyanine perchlorate; EPSC, excitatory postsynaptic current; EPSP, excitatory postsynaptic potential; IPSP, inhibitory postsynaptic potential; LGN, lateral geniculate nucleus (of the thalamus); PMBSF, posteromedial barrel subfield; RTN, reticular nucleus (of the thalamus); VB, ventrobasal nucleus (of the thalamus).

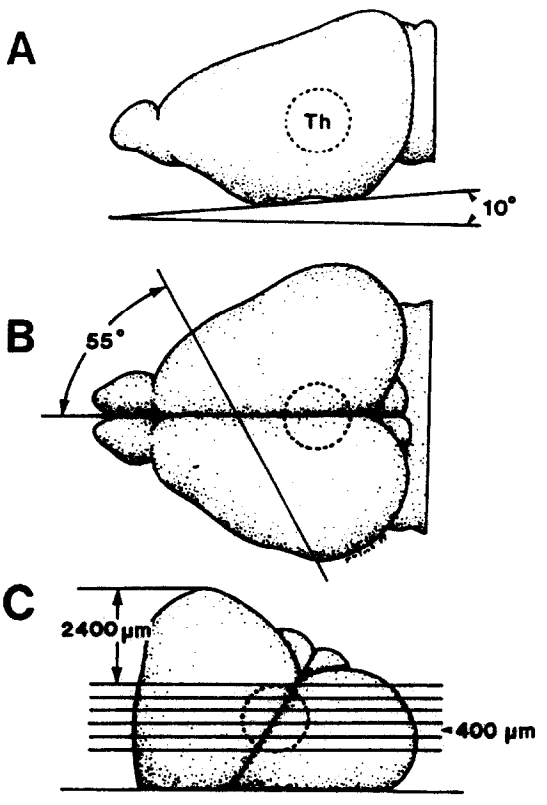

Fig. 1. Preparation of the thalamocortical slice. (A) Brain laid on the ramp. Th, approximate location of thalamus. (B) Dorsal view, showing angle of initial cut. (C) Brain on vibratome stage. Approximate position of collected slices. Typically two or three of these retained full thalamocortical connectivity, as defined in the text.

mixture. The ramp was placed on a protractor and a hand-held single edge razor blade was used to make a vertical cut through the tissue at an angle of 55° to the right of the posterior-to-anterior axis of the brain, intersecting this axis at about its anterior one-third point (Fig. 1B). The plane of cut was thus determined by two angles: the ramp tilt angle of 10° and the blade rotation angle of 55°. The tissue rostral to the cut was discarded. The remaining tissue was lightly blotted on filter paper and glued with cyanoacrylate glue onto the stage of a Lancer Vibratome with the cut surface down and the pial surface toward the blade. A small cube of agar was glued to the stage at the back of the tissue as a support against blade pressure. The glue was allowed a few seconds to dry and then the tissue was totally immersed in cold ACSF. Two or three (depending on brain size) slices 800-μm-thick were cut and discarded. The remaining tissue was cut (using very slow speed and high vibration amplitude settings) into 400-μm-thick slices (Fig. 1C) which were collected with a soft brush and suspended in sequence in ACSF-filled wells of a multi-well dish kept on ice. Slicing was terminated when the lateral ventricle (recognized by its pink tint) could no longer be seen on the surface of the tissue. The slices in the wells were briefly examined under a stereomicroscope while transilluminated from below. The three to four slices that exhibited uninterrupted fiber bundles traversing the corpus striatum were placed on small circles of filter paper moistened with ACSF, and incubated at room temperature in a moisturized O_2–CO_2 atmosphere for at least 1 h. The incubation period improved slice viability and in addition flattened the slices, preventing them from curling once transferred to the recording chamber.

Electrophysiological recordings

Extracellular recordings were done at room temperature, in a submersion-type chamber modified from published designs.[30,37] In our chamber the slices were placed in a well with a translucent bottom made of a 25-mm diameter glass coverslip. This allowed illumination of the slice from below at any chosen angle, using a fiber-optic light guide mounted on a rotatable holder. The angle of illumination was adjusted under visual control until optimal visualization of barrels and other structures was achieved (see Results). Slices in the recording chamber were continuously superfused with ACSF (1–2 ml/min). Slices could typically be maintained for 10–12 h after dissection without any appreciable deterioration of responses. Recordings were done using thin-wall glass micropipettes with a tip broken under microscopic control to about 5 μm diameter, and filled with a solution of physiological saline. Direct current resistance was typically 2–3 MΩ. The pipette tip was dipped (after filling) in black Indian ink to aid in its visualization. Extracellular stimulation was done by applying 100–200-μs cathodal pulses (3–15 V) through monopolar tungsten microelectrodes.

Intracellular recordings were done in an interface chamber maintained at 32°. Recording pipettes (1 mm o.d., 0.5 mm i.d. capillaries) were pulled on a Brown–Flaming puller, filled with 4 M potassium acetate and bevelled to about 200 MΩ resistance. Data were recorded on an FM tape (Racal Store 4DS, half-amplitude cut-off at 2.5 kHz) or, in later experiments, acquired via a microcomputer-based acquisition system (10 kHz sampling rate), and analysed off-line.

Current-source density analysis

Two simplifying assumptions were used in this analysis: (1) current flows only radially, i.e. there are no significant voltage differences as one moves laterally within one laminar position, an assumption largely consistent with our observations; and (2) the extracellular resistivity in the cortex along the radial direction is constant (see Ref. 35 for a justification of these assumptions and for a discussion of the consequences of their failure). With these assumptions, the current sources and sinks are directly proportional to the second spatial derivative of the voltage along the radial dimension.[36] This derivative was evaluated as follows: extracellular field potentials were recorded at 100-μm intervals along a line perpendicular to the pial surface. From each recording site, five to 10 traces were averaged. At the end of the series the electrode was returned to a few of the previous positions to verify that there had not been any significant changes in the response waveforms during the recording session. A difference trace was calculated from each pair of adjacent recording sites, and the process was repeated on the resultant waveforms. Data were recorded on an FM tape (Racal Store 4DS, half-amplitude cut-off at 2.5 kHz) and analysed off-line using a Nicolet 2090 digital oscilloscope.

Solutions

Normal ACSF was composed of (in mM): NaCl, 124; KCl, 5; NaH_2PO_4, 1.25; $MgSO_4$, 2; $CaCl_2$, 2; $NaHCO_3$, 26 and dextrose, 10. To block synaptic transmission, the ACSF contained (in mM): NaCl, 132; KCl, 5; $CaCl_2$, 0.5; $MgCl_2$, 2; $MnCl_2$ or $CdCl_2$, 2; $NaHCO_3$, 26; dextrose, 10.

Histology

Slices intended for Nissl staining were fixed overnight at 4°C in 4% paraformaldehyde and 30% sucrose in phosphate buffer (pH 7.4) and cut on a freezing microtome into 50-μm sections. Sections were mounted on slides, stained with Cresyl Violet and cleared using conventional histological protocol. For Di-I staining,[18] slices were fixed overnight at 4°C in 4% paraformaldehyde in phosphate buffer, laid on a glass slide, blotted lightly and a few particles of Di-I

[Di-IC_{18}(3), Molecular Probes, Inc.] were placed under microscopic control over the ventrobasal nucleus and pushed into the tissue with the aid of a fine needle. Slices were then placed in phosphate buffer and incubated at 37°C for one to two weeks. Slices were subsequently visualized in whole-mount with a Bio-Rad confocal scanning fluorescence microscope.

RESULTS

Visualization of barrels in living unstained slices

Barrels in rodent somatosensory cortex have previously been described only in fixed and variously stained tissue.[25–27,40,53,55] However, we found that barrels can be visualized just as well, and at times better, simply by transilluminating unstained, living slices with a fiber-optic light guide. Achieving optimal visualization required some trial and error in adjustment of the illumination angle; the barrels were best illuminated with the light beam incident at a slightly oblique angle (about 30° from vertical). A living unstained slice photographed in the recording chamber is illustrated in Fig. 2A. Layer IV appeared as a dark band interrupted by stretches of hollow rectangles. Nissl staining of representative slices demonstrated a one-to-one correspondence between these rectangles and the cytoarchitecturally defined barrels (Fig. 3A,B). In previous studies a tangential plane of section was used to demonstrate the striking two-dimensional pattern of the barrel-field.[55] We therefore sectioned a few brains in a plane parallel to the surface after flattening the cortex lightly between two glass slides. Indeed, in such slices transillumination revealed dark polygons arranged in the well-known pattern of the barrel-field (Fig. 2B). Nissl staining again confirmed that these polygons corresponded to cytoarchitecturally defined barrels (Fig. 3C,D). Henceforth we shall use the term "barrels" to designate both the cytoarchitectural structures seen in Nissl staining and the corresponding structures seen in the transilluminated, unstained slice.

In most cases, discrete barrels could be observed only in the central mediolateral third of the slice; other stretches of layer IV either appeared uniformly dark, without any apparent parcellation into discrete rectangles, or were not discernible at all. On occasion two or more barrel-containing stretches of layer IV were separated by sections devoid of barrels. Such barrel-free regions probably corresponded to the "dysgranular" zones that interdigitate the barrel cortex.[15] The largest and best-defined barrels were usually found in the region directly above the fimbria and lateral ventricle, overlying the thickest fiber bundles in the striatum (Fig. 2A). This area most probably corresponded to the posteromedial barrel subfield (PMBSF), the cortical representation of the large whiskers.[55]

In many of the slices the junction of layer IV with layer II/III was not sharply defined but consisted of a dark "fuzz" (Figs 2A, 3A). In all of our slices a second dark band was clearly visible in the deeper layers of the cortex (Figs 2A, 3A, asterisks). When camera lucida drawings of unstained slices were compared with Cresyl Violet-stained sections taken from the same slices, the lower dark band was found to extend on both sides of the border of layers V and VI (Fig. 3A,B). The darkest section of this band was always found directly underneath the PMBSF barrels.

In addition to barrels, transillumination clearly revealed many other cortical and subcortical structures. Fiber tracts were especially prominent. In animals older than about two-and-a-half weeks they appeared dark, whereas in younger animals they were often translucent or partially so, presumably due to absence of myelin.[21] The ventrobasal nucleus (VB) appeared in the transilluminated slice as a dark, half-oval or kidney-shaped structure (Fig. 2A). Barreloid borders were not readily apparent in the plane described here, but were prominent when the VB was sliced in a plane with a medioventral-to-dorsolateral tilt (Fig. 3E,F). Thin fiber bundles traversing the external part of the VB in the lateral–ventrolateral direction created a streaked pattern normal to its long axis (Fig. 4A; these bundles are obscured in the photograph in Fig. 2A). Upon reaching the border of the VB and the reticular nucleus (RTN), the bundles made a sharp dorsally directed turn and disappeared from view; the RTN consequently formed a relatively translucent outer shell around the VB. Individual fiber bundles were visible again in the corpus striatum coursing radially outward, and could be followed at least until they crossed the internal lamina of the subcortical white matter. The largest bundles (and the densest concentration of bundles) in the striatum were found directly underneath the PMBSF.

The layer IV response and its components

When rodent parietal cortex slices are prepared in the conventional coronal plane, all fiber pathways between the cortex and subcortical structures are apparently truncated at the external lamina of the white matter. We therefore searched for a plane of section that would retain functional thalamocortical connectivity in the slice. In the preliminary report of this preparation[3] we described a plane that is 45° from coronal, i.e. midway between coronal and sagittal planes. That plane gave good results with animals three weeks of age or younger, but failed with older animals. This suggested that the path followed by the thalamocortical fibers diverged somewhat from the plane of section and that as the brain grew larger a smaller number of intact fibers could be retained within the given thickness of the slice. Consequently we tried to find a more accurate plane by making small systematic variations in the two angles that determine the plane of section, the ramp angle and the blade angle (see Experimental Procedures). Although a variety of planes in a rather large spatial angle around the original plane gave successful results in young animals (three weeks old or younger),

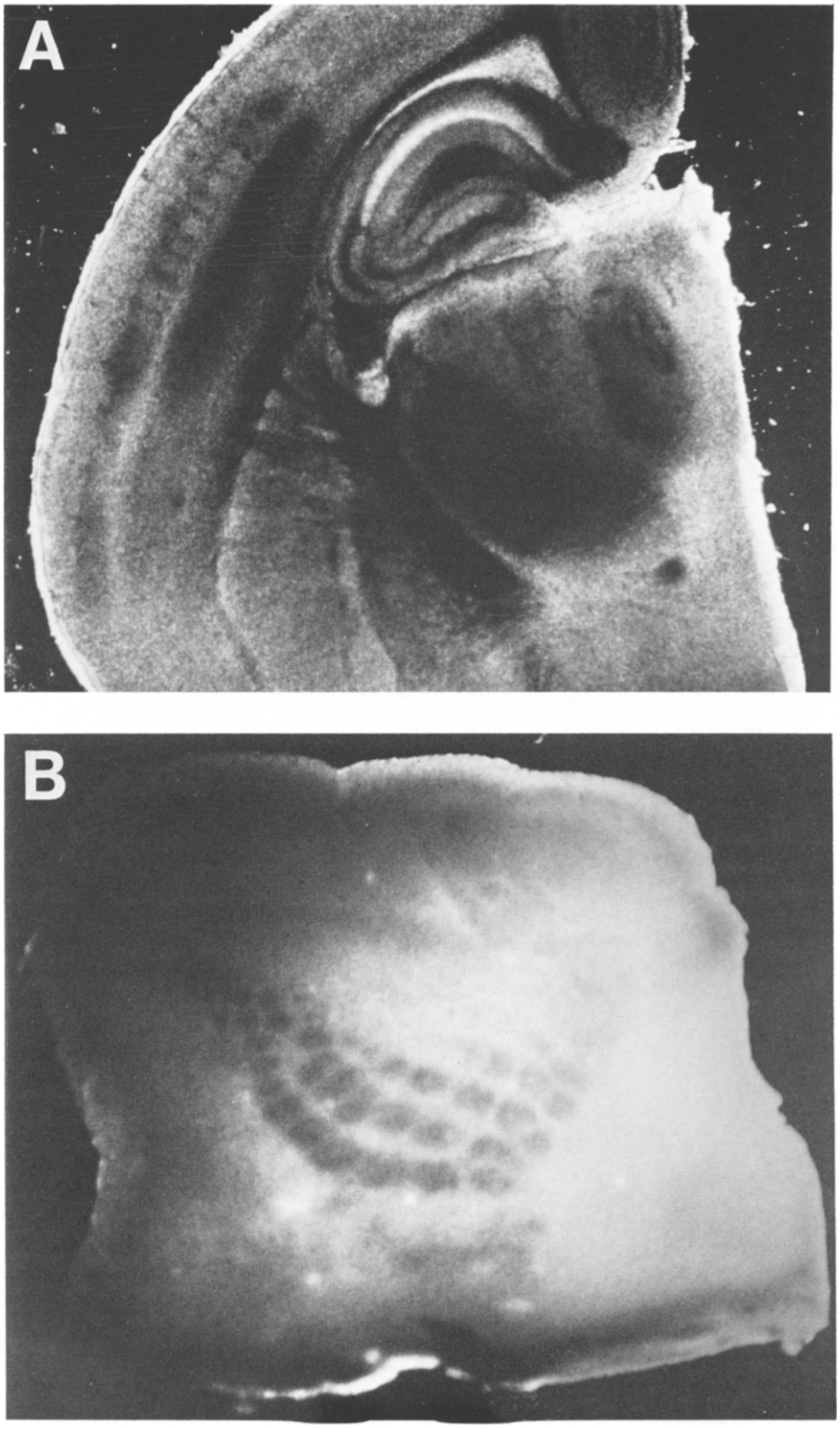

Fig. 2. Visualization of barrels in living unstained slices. (A) A thalamocortical slice photographed in the recording chamber. For identification of structures see Fig. 4A. (B) Tangential 200-μm-thick slice through lower layer III and upper layer IV. Four of the five rows of large posteromedial barrel subfield (PMBSF) barrels are clearly visible.

only the plane described above (Fig. 1) has so far worked consistently in older animals.

A slice was considered to have full thalamocortical connectivity if a focal electrical stimulus applied within the VB elicited an extracellular response in layer IV (see below for details). Recording such a response required careful positioning of the stimulating and the recording microelectrodes in relation to

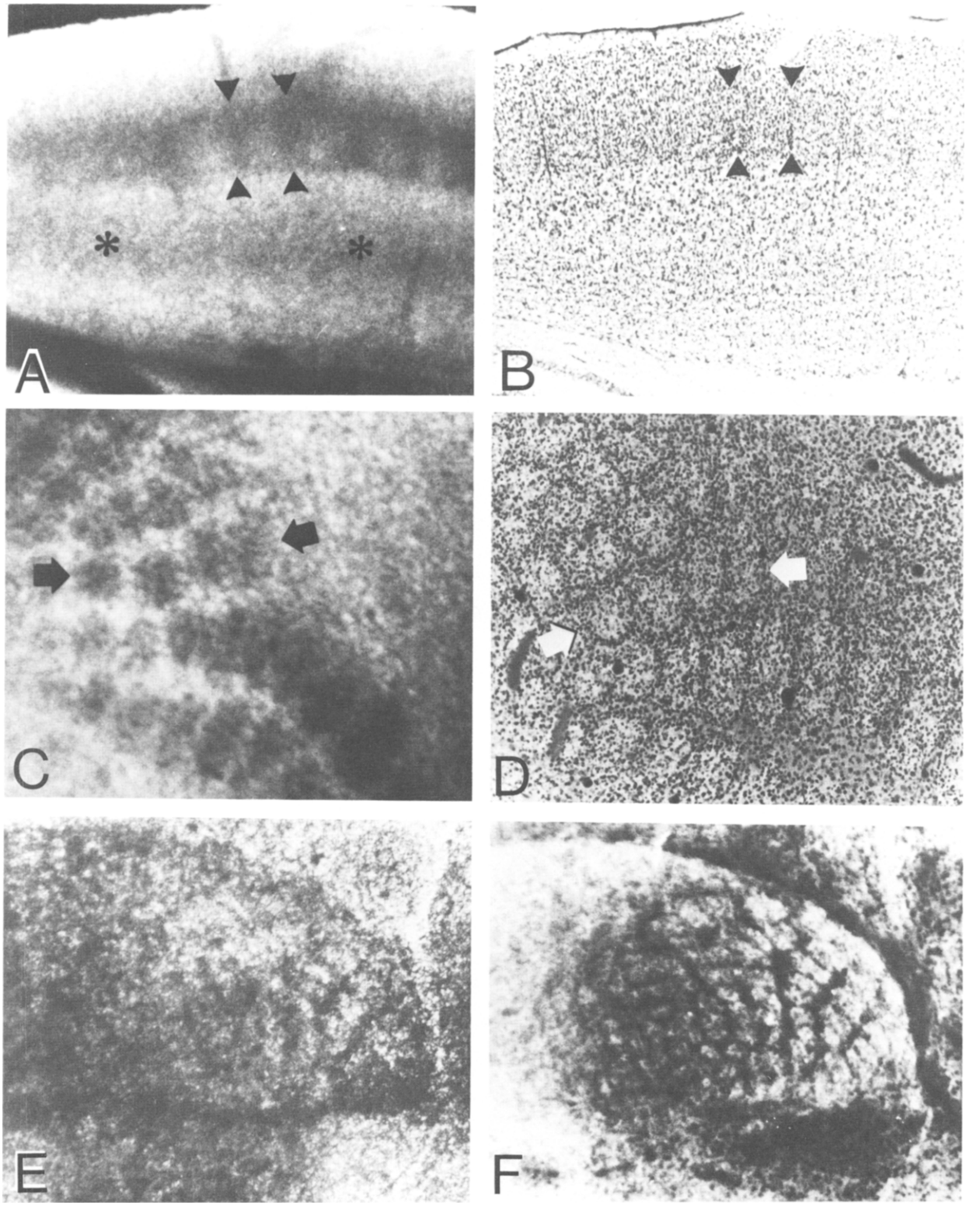

Fig. 3. Comparison between living unstained slices and Nissl-stained sections of barrel cortex and thalamus. Left panels (A,C,E) are living unstained slices (A and C are 400 μm thick; E is 200 μm thick) visualized by transillumination. Right panels (B,D,F) are 50 μm thick fixed and Cresyl Violet-stained sections taken from the corresponding slices at the left. Sections in D and F were photographed under epifluorescence illumination (rhodamine filters), a method that was found to enhance the barrel pattern. (A, B) Vertical section through the cortex. Arrowheads mark the same barrel in the unstained slice and in the stained section. (C, D) Tangential section through layer IV. Arrows mark same row of barrels. Note that in the unstained slice the barrel hollows are darker than the inter-barrel walls, but in the stained section the contrast is reversed. (E, F) Tangential section through the ventral basal nucleus (VB), approximately parallel to the plane of the vibrissae representation. Note the row of barreloids.

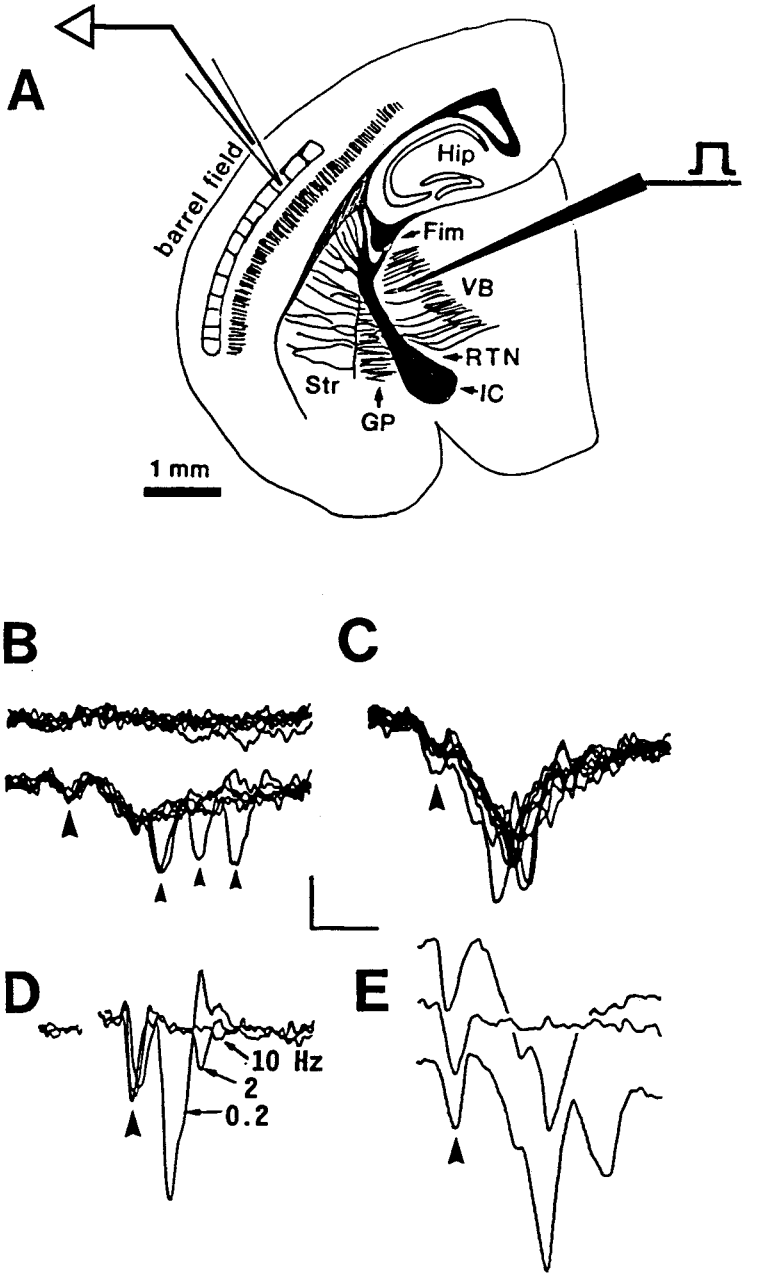

Fig. 4. Analysis of the thalamus-evoked responses in layer IV. (A) Typical position of the recording and stimulating microelectrodes marked on a camera lucida drawing of a thalamocortical slice. Dorsal is up, medial is right. Fim, fimbria; GP, globus pallidus; Hip, hippocampus; IC, internal capsule; Str, neostriatum. (B) All-or-none responses to a 0.2-Hz threshold stimulus (approx. 3 V). Failures (top) and successes (bottom) are plotted separately, six superimposed sweeps each. Note that the smallest evocable responses (lower traces) already consisted of two components, early (large arrowhead) and late, with single units sporadically superimposed on the late component (small arrowheads). (C) Extracellular responses in layer IV to a 0.2-Hz suprathreshold (approx. 12 V) stimulus in the VB, in the same slice and with the same electrode configuration as in B; 10 superimposed sweeps. Note early component (arrowhead). (D) Layer IV response at three different stimulation frequencies. The late component of the response was greatly attenuated at 2 Hz and abolished at 10 Hz, while the early component (arrowhead) was virtually unchanged. Three superimposed traces, each an average of six sweeps. (E) Thalamocortical responses before (top), during (center) and after (bottom) immersion in a low Ca^{2+}, high Mn^{2+} saline. Average of eight sweeps each. Note that the late component is abolished, the early component (arrowhead) unchanged under conditions that block synaptic transmission. Calibration bar is 2 ms, 0.2 mV (B,C); 4 ms, 0.1 mV (D); 2 ms, 0.1 mV (E). Sweeps in B, C and E start approximately 1.5 ms after stimulus onset. Positive is up for all traces.

each other, indicating the the response was due to activation of specific fiber pathways. The point of stimulation was generally within the external part of the VB near its border with the RTN, a region where large fiber bundles were clearly visible and could be targeted by the stimulating electrode (Fig. 4A); however, responses could usually be elicited from deeper within the VB as well. Typically two, and at most three, slices from one animal exhibited full thalamocortical connectivity. As expected, responses could also be elicited from points downstream of the VB along the pathway (e.g. internal capsule, neostriatum), but such responses were often contaminated with antidromic components (see below) and consequently such data were not included in the present analysis. Indeed, slices immediately adjacent to fully connected ones (as well as slices sectioned at unsuccessful planes) often exhibited partial connectivity: responses could not be elicited from the VB but could be elicited from points closer to the cortex. Such slices were not included here. It should be emphasized that, with the stimulus intensities used in this study, responses could not be elicited from sites within structures that are not known to project to the barrel cortex, such as the lateral geniculate nucleus (LGN) or the hippocampus, even when these sites were closer to the cortex (in absolute distance) than was the VB.

The response in the barrel cortex was largest, and most consistent in shape between slices, when recorded in layer IV proper or within the dark fuzz in lower layer III. We could not find any consistent dependence of the response waveform or amplitude on the exact position of the recording sites in relation to the barrels, i.e. whether it was within a barrel, between barrels or in dark regions of layer IV that lacked clearly defined barrels. When a stimulus of gradually increasing intensity was applied in the VB, a threshold for the appearance of a response in layer IV was typically reached at 3–4 V. The threshold response had an all-or-none character, with about half of the trials failing (top sweeps in Fig. 4B). The simplest explanation for this all-or-none property is that the response was generated either by a single fiber or by a small group of fibers with very close response thresholds. The successful trials (bottom sweeps in Fig. 4B) elicited a stereotypical waveform that consisted of two components that always appeared together: an initial small amplitude, short (typically 100 μV, 1 ms) negative deflection (large arrowhead) followed after about 1.2 ms by a larger and longer one. Superimposed on the second component, at variable latencies, were relatively large (300–400 μV) all-or-none negative events (small arrowheads). When the stimulus intensity was gradually increased, these all-or-none events appeared more frequently and at shorter and more consistent latencies, and eventually coalesced to form a single large amplitude (typically 0.5–0.8 mV) component (Fig. 4C). The response amplitude usually saturated at a stimulus level of 10–12 V.

The all-or-none events superimposed on the late component of the response had the characteristics of unitary action potentials; accordingly we hypothesized that the late component itself was an excitatory postsynaptic event and that the early component was the presynaptic spike volley arriving at the terminals. This hypothesis was corroborated by three independent tests.

High-frequency following. When stimulus frequencies were increased from the usual 0.2 Hz, the components of the response dropped out differentially (Fig. 4D). The late component was much reduced at 2 Hz, and failed completely at 10 Hz. The putative presynaptic component, on the other hand, persisted with little decrement at frequencies of at least 20 Hz and failed only at frequencies above 50–100 Hz.

Sensitivity to divalent ions. Perfusion for 5–10 min with a low Ca^{2+}, high Mn^{2+} (or Cd^{2+}) ACSF, a solution known to block synaptic transmission in neocortex,[11] invariably abolished the late component, with little or no change in the early one. The response recovered fully 20–30 min after a change back to control solution (Fig. 4E).

Sensitivity to amino acid antagonists. Kynurenic acid is a relatively nonspecific excitatory amino acid antagonist.[47] Adding 2 mM kynurenate to the perfusate totally blocked the late component but only slightly diminished the early one (data not shown). Responses recovered upon return to control solution.

Laminar profile of ventrobasal nucleus evoked responses in the barrel cortex

The laminar structure of the cortex lends itself well to a one-dimensional current-source density (CSD) analysis, a method which uses the extracellular voltage profile to infer the laminar distribution of the underlying current sinks and source.[36] The location and time-course of current sources and sinks is more meaningful than the voltage profile alone, since it can be interpreted directly in terms of the underlying electrical events at the cellular level. Specifically, within neocortex excitatory postsynaptic currents (EPSCs) and synchronous spiking are considered to be the main generators of extracellular current sinks.[35] A representative experiment is shown in Fig. 5. The left column is a series of extracellular field potentials recorded sequentially at 100-μm intervals through the depth of the cortex. The right column consists of the CSD traces corresponding to each of the recording sites except for the two outermost ones (these are excluded by the computation procedure). The largest current sinks were consistently localized in two specific laminar positions of the barrel cortex: in layer IV–lower layer III and on both sides of the layer V–VI border. These locations are precisely the sites of termination for the VB afferents,[17,21,22] and thus these sinks were probably a result of EPSCs

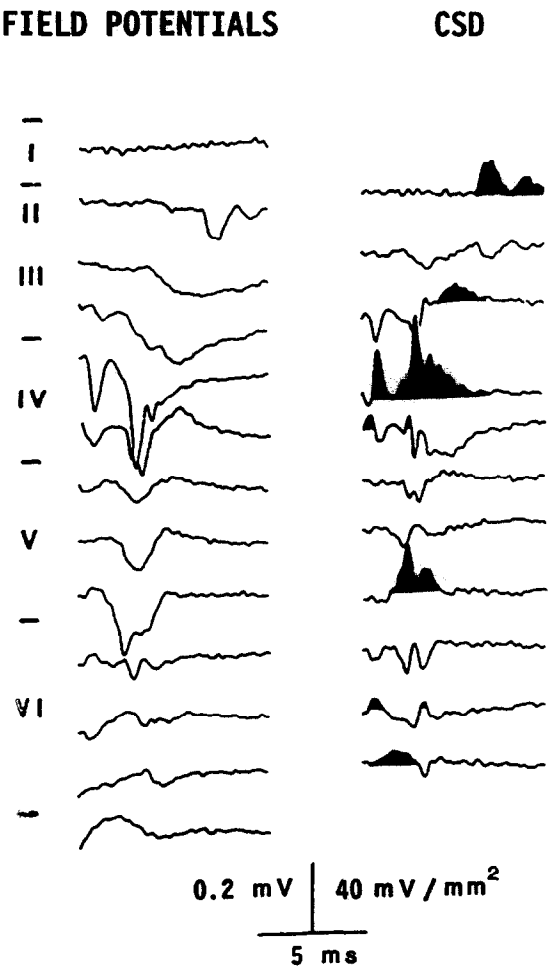

Fig. 5. Current-source density (CSD) analysis of the thalamocortical response. Left, profile of field potentials recorded at 100-μm intervals through the cortex. Each trace is an average of eight sweeps repeated at 0.2 Hz. Traces start 1.5 ms after stimulus onset. Positive is up. Right, CSD traces calculated from the voltage traces on the left; sinks (up) are shaded. CSD was calculated as follows: a difference trace was calculated from each pair of adjacent voltage traces, and the process repeated on the resultant traces. Note that the earliest and largest sinks are in layer IV and in the layer V–VI border. Later sinks are found in the supragranular layers. The "sink" in the bottom trace is derived from the stimulus artifact, which was more pronounced in the lower recording sites.

activated by the thalamocortical synapse, and/or of synchronous action potentials elicited in the postsynaptic cells. The large sink in layer IV was preceded by a smaller one that, as shown above, was of presynaptic origin, in all likelihood generated by the spike volley in the terminals. A similar (though less prominent) presynaptic sink often preceded the layer V/VI sink as well. A slow, long latency sink was usually observed in layer II/III, immediately above the large layer IV sink; however, the late events seen in Fig. 5 in upper layer II were not typical.

When the stimulating electrode was moved to the internal capsule or to the striatum we could often record, in the deep cortical layers, responses that had the characteristics of antidromically activated single units, i.e. all-or-none events that appeared at constant latency, could follow high frequencies of stimulation and whose waveform and amplitude were highly dependent on the recording position. However, such responses were never encountered when stimuli within the intensity range used in these experiments were applied in the VB proper.

Topographical organization in the ventrobasal nucleus-to-cortex projection

In vivo studies of the barrel cortex indicate that there is a one-to-one physiological mapping between the vibrassae and the barrels.[49] However, in our experiments the thalamocortical response was not restricted to one barrel. When moving the electrode laterally in layer IV while keeping the stimulating electrode stationary, the recorded response changed only a little over the extent of at least three barrels, and then gradually declined to zero amplitude over several more barrel-widths to either side. Similarly, when the recording microelectrode was kept stationary and the stimulating electrode was moved perpendicular to the direction of the thalamocortical fiber bundles in either VB or the striatum, a response in a given recording position could be elicited from several neighboring fiber bundles. The width of this "receptive field" was larger in the neostriatum than in the VB (Fig. 6A). A likely explanation for this topographical smear is that the thalamocortical axons reshuffle their positions along their course. In other words, in a single fiber bundle traversing the striatum one can encounter axons destined for several different (and probably adjacent) barrels and, vice versa, axons that are destined for a single barrel can be encountered in several adjacent fiber bundles. However, part of this apparent loss of order could have been due to current spread at the stimulation site, and lacking an independent estimate of the effective radius of this spread we could not quantify the extent of axonal reshuffling. We could, however, use such mapping experiments to arrive at conclusions about the gross topographical organization of the pathway. In the experiment depicted in Fig. 6A the recording electrode was positioned in sequence in different horizontal sectors of layer IV, and stimulation sites in both the VB and striatum that gave rise to measurable responses in the cortex were mapped for each recording site. The results showed that, although there was a significant overlap between the response-eliciting regions of adjacent recording sites, on average there was an orderly progression in the VB-to-cortex mapping, with more ventral or more dorsal points in the VB projecting to, respectively, more ventral or more dorsal points in the barrel-field.

Intracellular thalamocortically evoked responses

Although CSD analysis can point to the laminar location of synaptic events, it cannot identify their

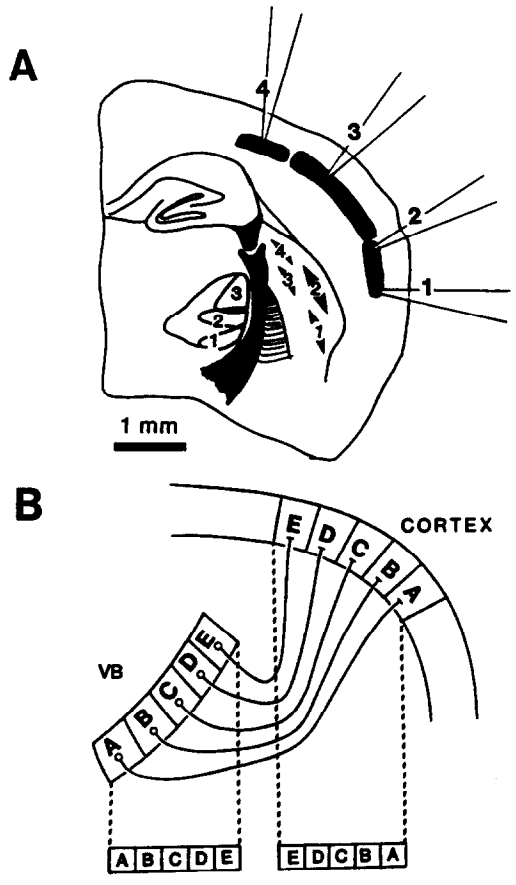

Fig. 6. The topographical organization of the thalamocortical projection. (A) A camera lucida outline of the slice. Barrel regions in layer IV are represented as solid black. Dorsal is up, medial is left. A recording electrode was kept stationary in each of four different points within layer IV (numbered), while a constant-amplitude stimulus was applied at various points in the striatum and in the VB. The range of stimulus locations from which a response could be elicited is marked for each recording point. Ranges in the striatum are marked by arrowheads and ranges in VB are represented as enclosed, numbered areas. Note that the mapping is area-to-area rather than point-to-point, but that the dorsoventral relation is preserved. (B) A highly schematic diagram of the thalamocortical pathway viewed in the plane used in these experiments. Note that when projected onto the horizontal plane, the cortical and thalamic maps appear to be mediolateral inversions of each other.

cellular substrates. The identity of the postsynaptic cell that gives rise to these EPSCs can at present be determined only by intracellular recording techniques. Fortunately the *in vitro* preparation is particularly amenable to this. We activated the thalamocortical pathway by a focal stimulus in VB, while monitoring the evoked field potential in layer IV and recording intracellularly from neurons in the barrel cortex. Figure 7 illustrates representative recordings from two cells, one in lower layer V (Fig. 7A) and the other in layer II/III (Fig. 7B). The responses of both cells to suprathreshold current steps identified them as regular-spiking cells (not shown), a distinct physiological class of cells with pyramidal morphology.[31] The top trace in both panels is the layer IV field potential, on which the onset of the presynaptic volley is demarcated by an arrowhead. The two traces below the field potential are the averaged intracellular responses. The membrane potential was held at two different levels by injection of constant current. The lower of the two intracellular traces is the response at a hyperpolarized potential and the upper trace is the response at a depolarized potential, just below firing threshold. Curved arrows mark the onset of synaptic events. At a hyperpolarized membrane potential a long-duration depolarizing synaptic response appeared at short-latency (0.6 ms from the presynaptic volley) in the infragranular cell and at a longer latency (2.1 ms) in the supragranular one. Based on the records alone one cannot determine conclusively the nature of the responses, since both excitatory postsynaptic potentials (EPSPs) and inhibitory postsynaptic potentials (IPSPs) can be positive-going at hyperpolarized membrane potentials; however, the upper traces in both panels, taken at a depolarized membrane potential, provide the diagnostic evidence. The response of the layer V cell was still positive-going initially but reversed polarity about 1.4 ms after its onset and became negative-going, thus revealing it to be an EPSP followed by an IPSP. In contrast, the response of the supragranular cell reversed almost at its onset, and was thus a relatively pure IPSP. The latency of the EPSP was equal to the latency of the extracellular postsynaptic response, in agreement with our interpretation that the latter arises from the thalamocortically evoked EPSCs, most probably monosynaptically. The latency to the IPSPs suggests that they were disynaptic, generated by intracortical interneurons that were themselves monosynaptically excited. A detailed description of the responses of barrel cortex neurons to both thalamocortical excitation and intracellular current steps, and the correlation between the two, will be presented in a companion paper (Agmon and Connors, unpublished observations).

Dioctadecyl-tetramethylindocarbocyanine perchlorate staining of the thalamocortical pathway

In order to confirm anatomically the presence of thalamocortical afferents in our slices, we fixed a few of the slices at the end of the recording session and placed several particles of the lipophilic dye Di-I[18] into the VB. The dye was allowed to diffuse at 37°C for one to two weeks and the slices were viewed with a confocal scanning fluorescence microscope. Figure 8 is a representative example. The fluorescent image was reversed to create a black-on-white picture. The internal capsule and fiber bundles coursing through the striatum were intensely fluorescent (Fig. 8B). Dense fluorescence was also found in layer VI and lower layer V, and consisted mainly of labeled cell bodies and dendrites, as revealed in high-power confocal images (not shown). These were probably

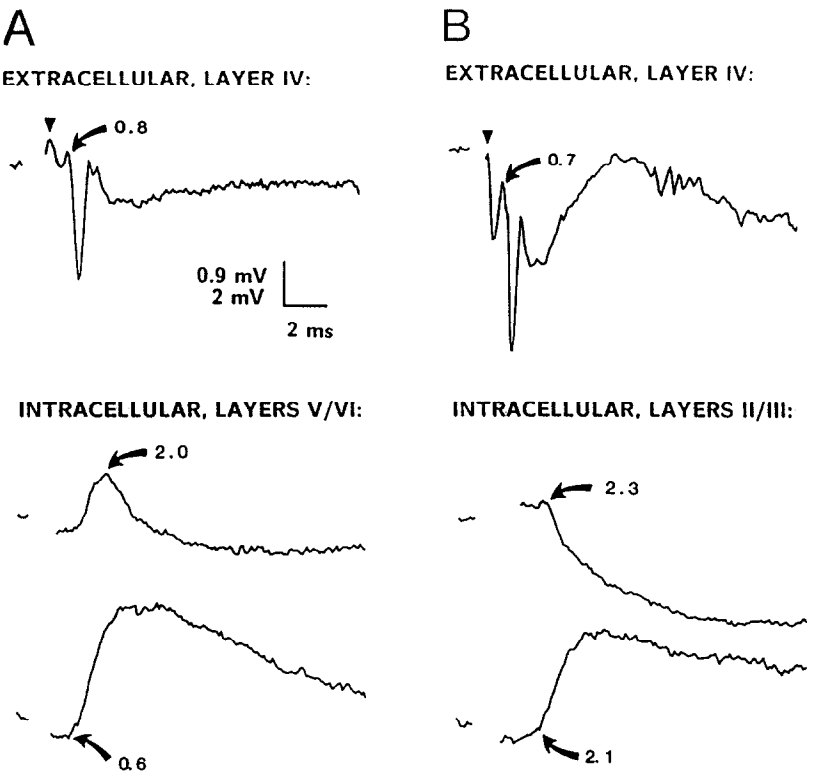

Fig. 7. Synaptic reponses of two barrel cortex cells to VB stimulation. (A) Simultaneously recorded responses, intracellularly from a layer V/VI neuron (bottom) and extracellularly from layer IV (top). (B) Simultaneously recorded responses from a different slice, intracellularly from a layer II/III neuron (bottom) and extracellularly from layer IV (top). Both cells were identified as regular-spiking (presumed pyramidal[31]) cells by their firing pattern in response to an intracellular current-pulse. The stimulus in each case was a single shock to the VB; stimulus artifacts have been blanked out. The onset of the field potential components representing the presynaptic volleys are marked by arrowheads. The two intracellular records shown for each cell were recorded at different membrane potentials (maintained by constant current injection): in each case the top trace is just below firing threshold and the lower trace is at a relatively hyperpolarized potential. Onset of each postsynaptic potential is marked with a curved arrow, together with its latency (in ms) from the presynaptic volley. Vertical distance between traces is arbitrary. All traces are an average of eight sweeps. Upper voltage calibration applies to the extracellular records, lower to the intracellular ones.

retrogradely labeled corticothalamic projection cells.[50] In layer IV (Fig. 8A, region between arrowheads) the fluorescent label had the patchy appearance characteristic of the barrel system. High-power confocal images revealed that each patch consisted of a dense plexus of axonal fibers.

DISCUSSION

The major new result reported here is the development of a preparation that allows selective activation of a thalamocortical pathway *in vitro*. This has not been possible previously for two reasons. Firstly, cutting slices in the conventional coronal plane of section seems to sever all axons leaving or entering the cortex, with the possible exception of callosal axons.[3,46] Secondly, unlike structures such as hippocampus or cerebellum, in which it is often possible to activate selectively a specific afferent or efferent pathway by correct placement of the stimulating microelectrode, in the neocortex intrinsic axons form such a dense network that a stimulus in virtually any intracortical location will activate intrinsic elements (axons and somatodendritic membranes) together with afferent fibers. A few *in vitro* studies of rodent visual cortex[44] have attempted to overcome these difficulties by placing the stimulating electrodes in the subcortical white matter, where some separation of afferent and efferent fibers has been suggested to exist.[54] To our knowledge such separation has not been shown to exist in the somatosensory cortex.

Another new finding described here is that barrels in rodent somatosensory cortex can be visualized in living, unstained slices by transillumination. Others have used transillumination as a means to visualize anatomical structures in freshly cut tissue,[13] but to the best of our knowledge this is the first study to describe its use for visualizing barrels. This method can be applied to a variety of ends in physiological, anatomical and developmental studies of the barrel cortex, in particular when fixation and dehydration artifacts are to be avoided. Moreover, combining the

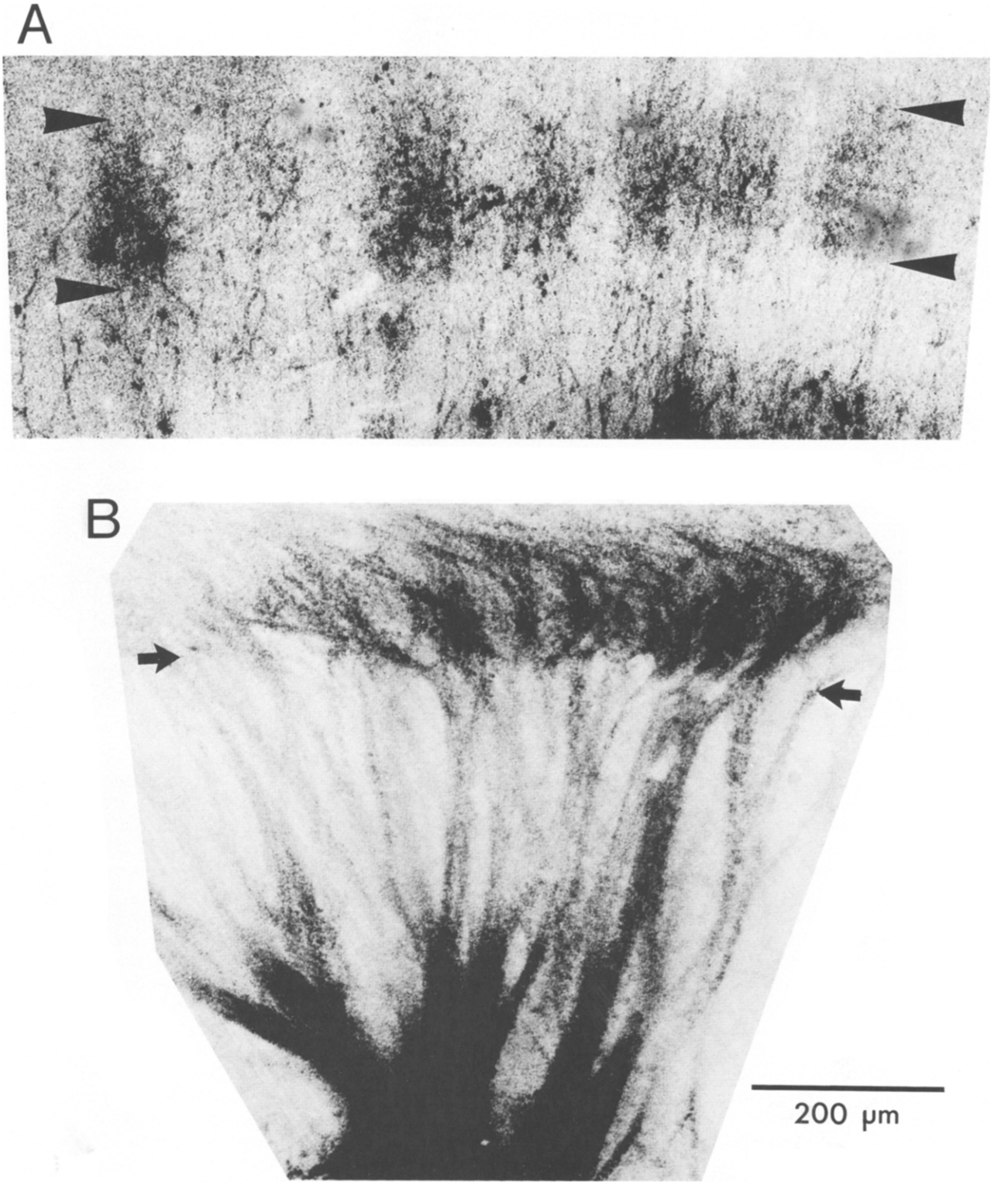

Fig. 8. Di-I staining of the thalamocortical pathway. (A) Di-I-stained terminals in layer IV. Arrowheads show laminar boundaries. Stained structures include axonal plexuses (afferent and possibly also intrinsic collaterals) in layer IV and lower layer III, and apical dendrites in upper layer V and in layer IV. (B) Di-I-stained axons in the internal capsule and subcortical white matter. The boundary of the striatum and white matter is shown by the arrows. Dye particles were placed in the VB (outside of the frame of the figure, at bottom) and the dye diffused through continuous axonal membranes into the cortex. Images were made with a confocal laser-scanning fluorescence microscope; contrast was digitally reversed to form a negative image, and pixel intensity values were digitally equalized within each section. The absolute fluorescence intensities were several orders of magnitude higher in the region shown in B than in that of A.

direct visualization achieved by transillumination with the ability to activate the thalamocortical pathway yields a particularly powerful experimental system.

Alternative interpretations of our data

The Di-I experiments clearly demonstrated that our slices retained many intact thalamocortical afferents. This is the only reasonable explanation for the labeled terminal patches in layer IV following dye placement in the VB. However, in order to establish our claim that we have selectively activated these axons, two alternative possibilities need to be eliminated. The first is that the responses were due to nonspecific current spread into the cortex. The second is that the responses were elicited by other pathways, specifically by collaterals of corticothalamic axons.

Although we have not attempted to measure directly the extent of current spread in our experiments, several indications suggest that it was small and did not account for any of our results. The fact that only slices cut at a very specific plane could generate responses upon VB stimulation suggests that no current spread to the cortex occurred; nonspecific current spread, had it existed, would have occurred at any plane of section. Indeed, we believe that current did not spread significantly beyond the VB, since moving the stimulating electrode to a location outside of the pathway, even if only a few hundred micrometers away (e.g. from the VB to the LGN or to the hippocampus), resulted in loss of the response. Even within the VB the effective radius of stimulation seems to have been rather small, as demonstrated by Fig. 6A: a movement as small as 200 μm laterally with the stimulating electrode was sometimes enough to cause loss of response in a given recording site.

It is somewhat more difficult to rule out the possible involvement of antidromically activated corticofugal axons. It is unlikely that any cell bodies in layer IV were activated antidromically, since all known corticofugal projections in the rodent originate in layers V and VI.[52] However, pre- and postsynaptic sinks in layer IV could still have been mediated by antidromic activation of corticothalamic fibers, as these axons are known to possess a rather dense collateral axonal arbor in layer IV[16,32,51] and thus could have contributed to the observed pre- and postsynaptic sinks in that layer. Indeed, our Di-I experiments show many retrogradely stained corticothalamic cells in layers Vb–VIa, implying that our plane of section preserved not only intact thalamocortical afferents but also intact corticothalamic axons, and these could have been activated by our stimuli in the VB; however, we consider this possibility unlikely. If corticothalamic axons were activated we should have encountered antidromic activity when recording in layers V and VI but, as mentioned above, we never encountered such activity either during extracellular recordings or during intracellular impalements when the stimulating electrode was positioned within the VB proper. Our failure to elicit antidromic responses from the VB suggests that our stimulus intensities were too low to activate the small-diameter terminals of the corticothalamic axons.[24] High thresholds for activation of corticothalamic terminals were also found in the cat.[16]

Comparison with other preparations

Recent years have seen various attempts at reconciling two opposing experimental approaches in brain science: studying the nervous system in an intact and close-to-life state vs studying a reduced system that allows easier access to its inner workings. The thalamocortical slice merits comparison with two such attempts: the perfused brain *in vitro*[29] and the perfused brain *in situ*.[39] Both of these experimental systems overcome the main technical bottleneck in whole-animal recordings, that of tissue movement, by artificially perfusing the brain through its own vascular system, and at the same time offer the researcher an intact mammalian nervous system with its full complement of neuronal pathways. Their main drawback to date is the technical difficulty involved in their preparation and maintenance and their relatively short viability period. The thalamocortical slice occupies a middle ground; in comparison with the internally perfused preparations it retains more limited connectivity, but it is relatively uncomplicated to prepare and maintain. It offers the additional significant benefits of visualization and direct access to deep structures with microelectrodes and drugs.

Comparison with in vivo *studies*

The contribution of the afferent volley to the electrically evoked field potential in primary sensory cortical areas was already suggested by early studies *in vivo*. Perl and Whitlock[38] found that the early response in cat somatosensory cortex to an afferent volley consisted of a very short latency spike component followed after about 1 ms by a larger wave component. The short latency spike component could follow higher frequency stimulation and was more resistant to anoxia and anesthetics than the wave component and on these grounds was attributed to activity in afferent fibers, while the wave component was attributed to postsynaptic activity in cortical cells. Other studies reached similar conclusions in the cat visual cortex[8] and in all three sensory neocortices.[28] The results of the present study concur with these conclusions and provide more direct evidence for the presynaptic origin of the initial component.

Application of the CSD method to the neocortex *in vivo* was pioneered by Mitzdorf and Singer[33,34] in the cat and monkey visual cortices. The results of our CSD analysis in the rodent are in substantial agreement with theirs. All three studies find two presumably monosynaptic sinks, a large one in layer IV and a smaller one in the deep layers, and longer-latency sinks in the superficial layers. The main difference between our study and theirs is that in the

cat a prolonged late sink is found in layer V; a comparable sink is absent from the present study. This difference is most probably due to the reduced excitability of the *in vitro* preparation and the resulting loss of polysynaptic responses.

The topography of the thalamocortical map in the barrel system

Our mapping experiment (Fig. 6A) suggests that there is an extensive reshuffling of fibers along the route from the VB to the barrel cortex, although the exact spatial extent of this phenomenon cannot be determined on the basis of the present data for lack of a quantitative estimate of the effective radius of our stimuli. This finding is in full agreement with the findings of a recent anatomical study in the mouse[7] which demonstrated loss of nearest-neighbor relationships between the VB axons coursing toward the barrel cortex. That same study, however, also concluded that there is a dorsoventral rotation of the fibers, accounting for a "well-known 180° rotation in the mediolateral direction between thalamic and cortical maps." This conclusion is incompatible with our data. Our results show (Fig. 6A) that the thalamus-to-cortex projection preserves the gross dorsoventral relationship, i.e. more dorsally situated bundles in the VB project more dorsally in the cortex, and vice versa. Indeed, we do not see the need for invoking a dorsoventral inversion in order to explain a mediolateral one. To our understanding the mediolateral inversion results from the fact that the planes of representation in the VB in the barrel cortex are not parallel, but rather orthogonal to each other, due to the medioventral-to-dorsolateral tilt of the VB. The thalamocortical fibers accommodate this tilt by making a dorsally directed turn upon their exit from the VB and along their subsequent course through the neostriatum (see Fig. 4A), but preserve their relative dorsoventral order. The mediolateral inversion can be considered illusory—it is only apparent when the cortical and the thalamic maps are projected on a horizontal plane; when projected on a vertical plane both maps are in register. These spatial relationships are illustrated in Fig. 6B.

The significance of the thalamocortical slice preparation

The ability to activate the thalamocortical pathway *in vitro* has a twofold significance. Firstly, it offers the opportunity to study in detail the physiological and pharmacological properties of this synapse. *In vitro* studies have contributed substantially to our knowledge of the properties of the main synapses in the hippocampus.[5,14,23] We know far less about the properties of the thalamocortical synapse. This is especially regrettable, since the thalamocortical synapse is the sole gateway by which any sensory information reaches the neocortex, and consequently it plays a pivotal role in sensory perception. Secondly, a preparation that allows selective activation of the major input to the neocortex provides a much more faithful model of the neocortical circuit than has been previously available *in vitro*. The thalamocortical preparation can now be used to study both the "wiring diagram" and the integrative properties of this circuit in detail.

Acknowledgements—We thank Larry Cauller and Laurie Silva for critical reading of an earlier version of this paper, and Bruce McIver and Yael Chagnac-Amitai for their generous help with the preparation of the figures. The Di-I staining experiments and confocal imaging were carried out in the laboratory of Dr E. G. Jones at the University of California in Irvine, and we thank him for permission to use the data here. A.A. was supported by NIMH training grant MH17047; additional support for this study came from the Klingenstein Fund and NIH grants NS25983 and NS0127 to B.W.C.

REFERENCES

1. Agmon A. (1988) Intrinsic properties and synaptic connectivity of mouse barrel cortex neurons: correlation between firing patterns and thalamocortical inputs. Ph.D. dissertation, Stanford University.
2. Agmon A. and Connors B. W. (1984) Visualization of the barrel field in living rat neocortical slices. *Soc. Neurosci. Abstr.* **10,** 493.
3. Agmon A. and Connors B. W. (1985) The transcallosal and thalamocortical barrel-field slice; preserving extrinsic connections *in vitro*. *Soc. Neurosci. Abstr.* **11,** 705.
4. Agmon A. and Connors B. W. (1989) Repetitive burst-firing neurons in the deep layers of mouse somatosensory cortex. *Neurosci. Lett.* **99,** 137–141.
5. Andersen P. O. (1987) Properties of hippocampal synapses of importance for integration and memory. In *Synaptic Function* (eds Edelman, Gall and Cowan), pp. 403–429. John Wiley, New York.
6. Armstrong-James M. and Fox K. (1987) Spatiotemporal convergence and divergence in the rat S1 "barrel" cortex. *J. comp. Neurol.* **263,** 265–281.
7. Bernardo K. L. and Woolsey T. A. (1987) Axonal trajectories between mouse somatosensory thalamus and cortex. *J. comp. Neurol.* **258,** 542–564.
8. Bishop G. H. and Clare M.H. (1953) Sequence of events in optic cortex response to volleys of impulses in the radiation. *J. Neurophysiol.* **16,** 490–498.
9. Chapin J. K. (1986) Laminar differences in sizes, shapes and response profiles of cutaneous receptive fields in the rat SI cortex. *Expl Brain Res.* **62,** 549–559.
10. Chapin J. K. and Lin C. S. (1984) Mapping the body representation in the SI cortex of anesthetized and awake rats. *J. comp. Neurol.* **229,** 199–213.
11. Connors B. W., Gutnick M. J. and Prince D. A. (1982) Electrophysiological properties of neocortical neurons *in vitro*. *J. Neurophysiol.* **48,** 1302–1320.
12. Connors B. W. and Gutnick M. J. (1984) Neocortex: cellular properties and intrinsic circuitry. In *Brain Slices* (ed. Dingledine R.), pp. 313–340. Plenum Press, New York.

13. Cuello A. C. and Carson S. (1983) Microdissection of fresh rat brain tissue slices. In *Brain Microdissection Techniques* (ed. Cuello A. C.), pp. 37–126. John Wiley, New York.
14. Dingledine R. (1984) In *Brain Slices* (ed. Dingledine R.), pp. 87–112. Plenum Press, New York.
15. Donoghue J. P. and Wise S. P. (1982) The motor cortex of the rat: cytoarchitecture and microstimulation mapping. *J. comp. Neurol.* **212,** 76–88.
16. Ferster D. and Lindstrom S. (1985) Synaptic excitation of neurons in area 17 of the cat neocortex by intracortical axon collaterals of cortico-geniculate cells. *J. Physiol., Lond.* **367,** 233–252.
17. Frost D. O. and Caviness V. S. (1980) Radial organization of thalamic projections to the neocortex in the mouse. *J. comp. Neurol.* **194,** 369–393.
18. Godement P., Vanselow J., Thanos S. and Bonhoeffer F. (1987) A study in developing visual systems with a new method of staining neurones and their processes in fixed tissue. *Development* **101,** 697–713.
19. Herkenham M. (1980) Laminar organization of thalamic projections to the rat neocortex. *Science* **207,** 532–534.
20. Ito M. (1985) Processing of vibrissa sensory information within the rat neocortex. *J. Neurophysiol.* **54,** 479–490.
21. Jacobson S. (1963) Sequence of myelination in the brain of the albino rat. A. Cerebral cortex thalamus and related structures. *J. comp. Neurol.* **121,** 5–29.
22. Jensen K. F. and Killackey H. P. (1987) Terminal arbors of axons projecting to the somatosensory cortex of the adult rat. I. The normal morphology of specific thalamocortical afferents. *J. Neurosci.* **7,** 3529–3543.
23. Johnston D. and Brown T. H. (1984) Biophysics and microphysiology of synaptic transmission in hippocampus. In *Brain Slices* (ed. Dingledine R.), pp. 51–86. Plenum Press, New York.
24. Jones E. G. and Powell T. P. S. (1969) An electron microscopic study of the mode of termination of cortico-thalamic fibres within the sensory relay nuclei of the thalamus. *Proc. R. Soc. B* **172,** 173–185.
25. Killackey H. P. and Leshin S. (1975) The organization of specific thalamocortical projections to the posteromedial barrel subfield of the rat somatic sensory cortex. *Brain Res.* **86,** 469–472.
26. Kristt D. A. (1979) Somatosensory cortex: acetylcholinesterase staining of barrel neuropil in the rat. *Neurosci. Lett.* **12,** 177–182.
27. Land P. W. and Simons D. J. (1985) Cytochrome oxidase staining in the rat SmI barrel cortex. *J. comp. Neurol.* **238,** 225–235.
28. Landau W. M. and Clare M. H. (1956) A note on the characteristic response pattern in primary sensory projection cortex of the cat following a synchronous afferent volley. *Electroenceph. clin. Neurophysiol.* **8,** 457–464.
29. Llinás R. and Muhlethaler M. (1988) An electrophysiological study of the *in vitro* perfused brainstem–cerebellum of adult guinea-pig. *J. Physiol., Lond.* **404,** 215–240.
30. Llinás R. and Sugimori M. (1980) Electrophysiological properties of *in vitro* Purkinje cell somata in mammalian cerebellar slices. *J. Physiol., Lond.* **305,** 171–195.
31. McCormick D. A., Connors B. W., Lighthall J. W. and Prince D. A. (1985) Comparative electrophysiology of pyramidal and sparsely spiny stellate neurons of the neocortex. *J. Neurophysiol.* **54,** 782–806.
32. McGuire B. A., Hornung J. P., Gilbert C. D. and Wiesel T. N. (1984) Patterns of synaptic input to layer IV of cat striate cortex. *J. Neurosci.* **4,** 3021–3033.
33. Mitzdorf U. and Singer W. (1978) Prominent excitatory pathways in the cat visual cortex (A17 and A18): a current source density analysis of electrically evoked potentials. *Expl Brain Res.* **33,** 371–394.
34. Mitzdorf U. and Singer W. (1979) Excitatory synaptic ensemble properties in the visual cortex of the macaque monkey: a current source density analysis of electrically evoked potentials. *J. comp. Neurol.* **187,** 71–83.
35. Mitzdorf U. and Singer W. (1980) Monocular activation of visual cortex in normal and monocularly deprived cats: an analysis of evoked potentials. *J. Physiol., Lond.* **304,** 203–220.
36. Nicholson C. and Freeman J. A. (1975) Theory of current source-density analysis and determination of conductivity tensor for anuran cerebellum. *J. Neurophysiol.* **38,** 356–368.
37. Nicoll R. A. and Alger B. E. (1981) A simple chamber for recording from submerged brain slices. *J. Neurosci. Meth.* **4,** 153–156.
38. Perl E. R. and Whitlock D. G. (1955) Potentials evoked in cerebral somatosensory region. *J. Neurophysiol.* **18,** 486–505.
39. Richerson G. B. and Getting P. A. (1987) Maintenance of complex neural function during perfusion of the mammalian brain. *Brain Res.* **409,** 123–132.
40. Sandell J. H. (1984) The distribution of hexokinase compared to cytochrome oxidase and acetylcholinesterase in the somatosensory cortex and the superior colliculus of the rat. *Brain Res.* **290,** 384–389.
41. Simons D. J. (1978) Response properties of vibrissa units in rat SI somatosensory neocortex. *J. Neurophysiol.* **41,** 798–820.
42. Simons D. J. (1985) Temporal and spatial integration in the rat SI vibrissa cortex. *J. Neurophysiol.* **54,** 615–635.
43. Simons D. J. and Woolsey T. A. (1979) Functional organization in mouse barrel cortex. *Brain Res.* **165,** 327–332.
44. Vaknin G.and Teyler T. J. (1988) The *in vitro* visual cortical slice in rodent as a model system for studying cortical microcircuitry revealed by current source density analysis. *Soc. Neurosci. Abstr.* **13,** 1045.
45. Van der Loos H. (1976) Barreloids in mouse somatosensory thalamus. *Neurosci. Lett.* **2,** 1–6.
46. Vogt B. A. and Gorman A. L. F. (1982) Responses of cortical neurons to stimulation of corpus callosum *in vitro*. *J. Neurophysiol.* **48,** 1257–1273.
47. Watkins J. C. and Evans R. H. (1981) Excitatory amino acid transmitters. *Ann. Rev. Pharmac. Toxicol.* **21,** 165–204.
48. Welker C. (1971) Microelectrode delineation of fine grain somatotopic organization of (SmI) cerebral neocortex in albino rat. *Brain Res.* **26,** 259–275.
49. Welker C. (1976) Receptive fields of barrels in the somatosensory neocortex of the rat. *J. comp. Neurol.* **166,** 173–190.
50. White E. L. (1989) *Cortical Circuits: Synaptic Organization of the Cerebral Cortex—Structure, Function and Theory*, p. 223. Birkhauser, Boston.
51. White E. L. and Keller A. (1987) Intrinsic circuitry involving the local axon collaterals of corticothalamic projection cells in mouse SmI cortex. *J. comp. Neurol.* **262,** 13–26.
52. Wise S. P. and Jones E. G. (1977) Cells of origin and terminal distribution of descending projections of the rat somatic sensory cortex. *J. comp. Neurol.* **175,** 129–158.
53. Wong-Riley M. T. and Welt C. (1980) Histochemical changes in cytochrome oxidase of cortical barrels after vibrissal removal in neonatal and adult mice. *Proc. natn. Acad. Sci. U.S.A.* **77,** 2333–2337.

54. Woodward W. R. and Coull B. M. (1984) Localization and organization of geniculocortical and corticofugal fiber tracts within the subcortical white matter. *Neuroscience* **12,** 1089–1099.
55. Woolsey T. A. and Van der Loos H. (1970) The description of a cortical field composed of discrete cytoarchitectonic units. *Brain Res.* **17,** 205–242.

(*Accepted* 19 *September* 1990)